PH.D. RESEARCH PROPOSAL:

Numerical Investigation of Drop Impact on Liquid Pool

Somdeb Bandopadhyay

May 04, 2016

Supervisor:

Yi Ju CHOU

Institute of Applied Mechanics

National Taiwan University

Contents

List of Figures

1 Introduction

In this proposed research, we intend to develop a numerical framework to perform direct numerical simulation of multiphase flows and afterwards use it to analyse the interfacial instabilities in drop impact on liquid pool problem. The structure of this proposal is described here. In section 2, a brief introduction of the physical multiphase problem is given. Afterwards, the state of art of relevant numerical methods are discussed in section 3. In section 4, we try to provide a flowchart for this work and try to estimate the required time to properly finish this work. Lastly, section 5 covers the expected results from this research.

2 Drop Impact on Liquid Pool

The impact of drop on liquid pool is a classical problem in fluid mechanics. Depending on various factors [e.g. impact velocity of the drop, the depth of the target liquid and the physical properties of the fluids], the droplet can spread, float, coalesce, bounce, or splash[Rein (1993)] . for high impact velocity, during the early stage of drop impact, a typical fine jet often termed as 'ejecta sheet' is formed [Thoroddsen et al. (2008)] (more discussion in this regard is given in section 1.2). The bouncing of drop can occur on perturbed liquid surfaces. If the drop is able to rupture the thin-film of gas separating it from the liquid reservoir, it leads to coalescence. Finally, drop impact with higher energy (e.g high velocity) leads to splashing. In case of splashing, the impacting drop creates a crater in the fluid surface, which is followed by the formation of crown around the crater. Additionally, a central jet, called the 'Rayleigh jet' or 'Worthington jet' protrudes from the center of crater. For high-enough impact energy , the jet rises to the point where it pinches off, sending one or more droplets upward out of the surface. Bubble/air entrapment, formation of vortex rings etc are other physical after-effects of drop-impact on a liquid pool.

2.1 Motivation

A thorough understanding of the mechanisms associated with drop impact is of high importance for various practical applications.

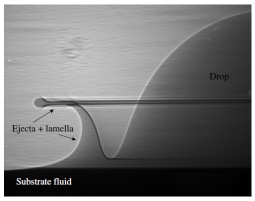

(a) The ejecta sheet
[Zhang et al. (2012)]

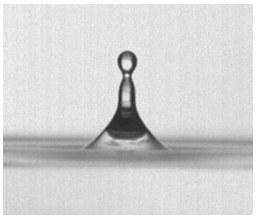

(b) Rayleigh jet
[Castillo-Orozco et al. (2015)]

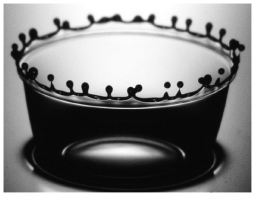

(c) A crown splash
[Zhang et al. (2010)]

Figure 1: Some typical phenomena corresponding to drop impact and splashing

In combustion related industrial applications, fuel droplets splashing on the walls are beneficial to the production of smaller droplets which leads to enhanced combustion [Moreira et al. (2010)]. On the contrary, in case of ink-jet printing , such splashing must be avoided to improve the precision.

Bubble entrapment phenomena is another crucial issue for ink-jet printing , as well as in spray coatings or liquid paints. The wide application of spray-coating in the pharmaceutical industry [Bolleddula et al. (2010)] , granulation [Marston et al. (2010)] ,cooling of hot surfaces in nuclear reactors [Sawan and Carbon (1975)], electronics industry [Kim (2007)] etc. leads to a high demand for the research on bubble entrapment dynamics.

From marine science perspective, the smallest splashed droplets during rain, can evaporate, leaving microscopic aerosols that can act as nucleation sites

during cloud formation, affecting climate [Wanninkhof et al. (2009)]. When the rain droplets impact on the ground, they participate in soil erosion. The splashed droplets can also contribute to the seeds or pore dispersal, and spreading of diseases and pesticides [Rossi and Caffi (2012)].

Last but not the least, the physics of droplet impact and corresponding splashing phenomena is important in criminal forensic to study blood splash patterns as noted by Hulse-Smith et al. (2005), Knock and Davison (2007).

2.2 Review of Previous Works

Due to the wide industrial application , drop impact problem has been one of the prime interest in fluid dynamics. The dynamic structures related to drop impact on liquid pool can be catagorized into two parts : early splash or ejecta sheet and late-time splash or conventional splashing.

The existence of ejecta sheet was a fundamental discovery in drop-impact dynamics, made during the last decade Weiss and Yarin (1999), Thoroddsen (2002), Josserand and Zaleski (2003). As mentioned in the introductory part, ejecta sheet is a fine jet which emerges from the neck that connects the drop to the pool for high impact velocities. From experimentalists' point of view, this phenomenon was undetected until recent advances in high-speed imaging [Thoroddsen et al. (2008)]. The ejecta sheet is the most significant factor for the splashing of micro-droplets. Among the numerical works, however, it was first observed in the simulations performed by Weiss and Yarin (1999). Similar

observations were reported by R. Davidson (2002). These studies did not include viscous effects in the boundary integral calculations, and thus, could not capture the topology changes that would have led to this kind of splashing and bubble entrapment. Different types of instability-mechanisms have been considered in the literature that could explain the early splashing mechanism, such as the Richtmyer-Meshkov instability [Gueyffier and Zaleski (1998), Krechetnikov and Homsy (2009)], the Rayleigh-Plateau capillary instability [Zhang et al. (2010)], combinations of both [Krechetnikov (2010), Agbaglah et al. (2013)] or waves in the ejecta-sheet [Villermaux and Clanet (2002)].

Late time splash is possibly the most studied phenomena corresponding to the drop impact dynamics. The research on splashing was pioneered by Worthington (1876, 1877, 1882, 1895). At first he used strobed visual observations and sketches. Afterwards he incorporated the use of nascent technology in photography and published the seminal book 'A Study of Splashes' [Worthington (1908)] . This work was followed by many experimental research in the subsequent century, incorporating the latest imaging technology of each time period. The earlier research was focused on the overall edge breakup of the corona, after it rises out of the pool, forming what is often called the Edgerton crown [Edgerton and Killian, 1939]. Numerous studies are dedicated to determine the splashing threshold, especially for impacts onto solid surfaces. Some of the noteworthy works in this aspect are those of Stow and Hadfield (1981) Mundo et al. (1995) and Cossali et al. (1997). These works proposed the

importance of the splashing parameter $K{=}We\sqrt{Re}$. The Reynolds Number [$Re = \frac{\rho UR}{\mu}$] and Weber-Number [$We = \frac{\rho RU^2}{\sigma}$] are calculated from the impact velocity of the drop U, the drop radius R, the density (ρ) and dynamic viscosity (μ) of the fluid, and the surface tension σ. Rioboo et al. (2001, 2003) have further characterized the different splashing scenarios and proposed the terminology of corona splash where the crown breaks up on its edge into droplets, vs. the prompt splash which arises at the very early contact of the drop with the solid substrate. Most instructive imaging of the early contact have been carried out for impacts onto glass surfaces, where the dynamics can be observed through the substrate[Thoroddsen and Sakakibara (1998)].

Recently Xu et al. (2005) have showed that onset of splashing can be delayed by reducing the air pressure. It has not been clearly determined what causes this, but some relevant studies suggest that it is related to the cushioning under the drop by the air layer [Smith et al. (2003), Mehdi-Nejad et al. (2003), Duchemin and Josserand (2011), Driscoll and Nagel (2011), Hicks and Purvis (2011), Palacios et al. (2012), Kolinski et al. (2012) and Liu et al. (2013)]. These theoritical foundations lead to the introduction of a new non-dimensional parameter, i.e. the density ratio of the gas (air) to that of the liquid.

Apart from splashing, the other physical phenomena related to drop-impact dynamics include the generation of sound [Prosperetti and Oguz (1993)], entrapped bubbles[Liow and Cole (2007)] and creation of vortex rings [Peck and Sigurdson (1994)] which can carry micro-bubbles into the fluid [Esmailizadeh

and Mesler (1986)]. Yarin (2006) and Thoroddsen et al. (2008) have discussed the complex dynamics related to splashing or entrapment of bubbles. The study of underwater sound from the impact of rain on a water surface eventually led to the study of bubble entrapment [Prosperetti and Oguz (1993)]. Franz (1959) discussed two different mechanisms which could be responsible for the sound produced by drop impacts. At the very moment when the drop impacts the surface, a sharp pulse of sound is emitted, known as the *water hammer* effect. The second mechanism involves the oscillation of the bubbles entrained in the water, which leads to the generation of sound. Pumphrey and Elmore (1990) described four different processes for bubble entrapment when a water drop impacts the surface of deep water, namely irregular Franz-type entrainment, regular entrainment, large bubble entrainment and Mesler entrainment [Esmailizadeh and Mesler (1986)]. Regular entrainment leads to the formation of a single bubble when the crater collapse , whereas either a multitude of tiny bubbles [Mesler entrainment: Esmailizadeh and Mesler (1986), Sigler and Mesler (1990), Pumphrey et al. (1989)] or only a few individual bubbles [Thoroddsen et al. (2003),Thoroddsen et al. (2012)] may be entrapped in the bulk fluid due to rupture of the thin air sheet remaining trapped between the contacting surfaces.

To understand the transition from drop-coalescence to splashing of drops alot of effort has been provided to the construct a proper regime mapping for different stages of drop-impact phenomena by means of theoretical arguments, experimental results and numerical simulation. In this context, non-dimensional

numbers are used to plot the transition map between different regimes. Apart from Reynolds Number (Re) and Weber number (We), most used non-dimensional parameters in this regard are Ohnesorge Number [$Oh = \frac{\mu}{\sqrt{\sigma\rho R}}$] , Bond number [$Bo = \frac{\Delta\rho g R^2}{\mu}$; g=gravitational acceleration], Froude Number [$Fr = \frac{U^2}{gR}$] and Capillary Number [$Ca = \frac{\mu U}{\sigma}$]. The boundaries for regular bubble entrainment regime were determined by Pumphrey and Elmore (1990) from the experimental data of normal impact of water drops on a plane water surface with high-speed photography. Afterwards, Rein (1996) identified the boundaries for jet formation by rearranging different flows according to the Weber number.He identified the presence of a vortex ring to be the signature coalescence and a secondary droplet to be the signature of splashing. The bubble entrapment zone was considered to be a special case of splashing. Few years later, Morton et al. (2000) performed both experimental and numerical investigations and conclusively showed the existence of capillary waves during bubble entrapment and the growth of a thin high-speed jet. They established the criterion for bubble entrapment as capillary wave propagation down the walls of the crater at a speed greater than that of crater collapse to form a thick Rayleigh jet. In his doctoral dissertation Cole (2007) presented a comprehensive drop splash map using PIV and high-speed video techniques. He has categorized the flow physics of liquid drop impact on a deep pool into six flow regimes. some of his observations include microbubble formation from floating drops, pre-entrapment jetting, multiple primary bubble entrapment and downward jets penetrating the

entrapped bubble. Deegan et al. (2007) considered distinct dynamical origins of the secondary droplets and constructed a regime map based on We and Re for crown splash. Agbaglah et al. (2015) and Ray et al. (2015) have numerically investigated different cases of drop-impact on liquid pool and have developed regime maps for vortex ring formation, bubble entrapment and jet formation based on We, Fr and Ca. Castillo-Orozco et al. (2015) has prepared a different type of regime map based on Re, Oh and We for crown splash and Rayleigh-jet breakup.

It should be noted that the selection of non-dimensional parameters to develop regime map depends on the type of problem and objective of the analysis. Also, so far, most of the numerical investigations are performed using spherical droplet size and ignoring heat transfer between droplet and the liquid pool. As such, despite of these previous works the possibility to contribute in this topic is still at large.

3 Numerical Approach : A Review

The numerical formulation of the multiphase drop-impact problem can be performed by Lagrangian method, Eulerian method or combination of both. The Lagrangian formulations lead to the use of moving, boundary conforming meshes for the interface. Considering the expected deformation of the interface in this case, such approach would be unwise to pursue. The Eulerian approach, on the contrary, can be applied on a fixed mesh framework. In addition to the resolution requirements, numerical simulations of drop-impact requires consideration of the discontinuous nature of the material properties at the interface and implementation of the singular surface tension force into the Navier-Stokes equations in a stable and accurate manner. The topology changes of the interface need to be tracked as well. Unfortunately, the length scale associated with topology changes (such as "pinch off" events) approaches zero which further necessitates the use of accurate modeling. Tryggvason et al. (2011) has reviewed the challenges to reproduce the drop impact phenomena on computational framework. In following sections, we shall briefly review the evolution and development of different numerical methods for multiphase flow problem. Detailed formulation of every method is beyond the scope of this review and only a generalized descriptions are provided here.

3.1 Early Works : The MAC Method

The oldest approach to numerically solve multiphase navier-stokes equation is the Marker-and-Cell (MAC) method developed at Los Alamos by Harlow and his collaborators to solve the free surface flow problems. In this method the fluid is identified by marker particles distributed throughout the fluid region and the governing equations are solved on a regular grid which covers both the fluid-filled and the empty part of the domain. Notably, although the prime objective to develop the MAC method was free surface flow problem, it was also the first method to successfully solve the Navier-Stokes equation using the primitive variables. The staggered grid used in this approach was a novelty at that time. The method was introduced in Harlow and Welch (1965) and two sample computations of the classical dam-breaking problem were shown in that first paper. Afterwards it was used by Harlow and Welch (1966) to examine the Rayleigh-Taylor problem and Harlow and Shannon (1967) to study the splashing phenomena. In the original implementation, the MAC method assumed a free surface and as such, only one fluid was under consideration. However, the Los Alamos group soon realized that the method can be applied to two-fluid problems. This revelation lead to the published work of Daly (1969b) where the author computed the evolution of the Rayleigh-Taylor instability for finite density ratios. Afterwards, surface tension was added by Daly (1969a) and the method was again used to examine the Rayleigh-Taylor instability. The MAC method quickly attracted a number of research groups who used it to study

several problems including free surface waves [Chan and Street (1970)], the oscillations of an axisymmetric droplet [Foote (1973)], the collision of a droplet with a rigid wall [Foote (1975)], and the collapse of a cavitation bubble [Chapman and Plesset (1972); Mitchell and Hammitt (1973)].

3.2 VOF Method

The next generation of methods for multiphase flows evolved gradually from the MAC method. It was noted in the work by Harlow and Welch (1965) that the marker particles could cause inaccuracies. As a result, the particles were replaced by a marker function and the Volume-of-Fluid (VOF) method was born. VOF was first discussed in the published work of Hirt and Nichols (1981) but the approach was already used in previous works [De Bar (1974); Noh and Woodward (1976)]. A cell-averaged marker function was used To resolve the issue of numerical diffusion while advecting a sharp marker function. Moreover, the interface is "reconstructed" in the VOF method in such a way that the marker does not start to flow into a new cell until the current cell is full. In the early implementation of VOF, the interface in each cell was simply assumed to be a vertical plane for advection in the horizontal direction and a horizontal plane for advection in the vertical direction. This relatively crude reconstruction often lead to large amount of "floatsam and jetsam" (small unphysical droplets that break away from the interface) that degraded the accuracy of the computation. To improve the representation, Youngs (1982), Ashgriz and Poo (1991) and others introduced

more complex reconstructions of the interface, representing it with a line (two dimensions) or a plane (three dimensions) that could be oriented arbitrarily in such a way as to best fit the interface. This increased the complexity of the method considerably but resulted in greatly improved advection of the marker function. However, even with higher-order representation of the fluid interface in each cell, the accurate computation of surface tension remained a major problem. This problem was countered by Brackbill et al. (1992) who showed that the curvature (and hence surface tension) could be computed by taking the discrete divergence of the marker function. A "conservative" version of this "continuum surface force" method was developed by Lafaurie et al. (1994). The VOF method has been improved in various ways by a number of authors. Apart from better reconstruction scheme for the interface [Rider and Kothe (1998); Scardovelli and Zaleski (2000); Aulisa et al. (2007)] and computation of the surface tension [Renardy and Renardy (2002); Popinet (2009)], more advanced advection schemes for the momentum equation and better solvers for the pressure equation have been introduced [e.g Rudman (1997)]. Other improvements of VOF method includes the use of sub-cells to keep the interface as sharp as possible [Chen et al. (1997)].

Being one of the oldest methods, VOF has been thoroughly investigated over past years to seek possible improvements. Among the most comprehensive reports in this context, the works by Rudman (1997) Rudman and by Gopala and van Wachem (2008). In both papers the ability to keep the interface sharp and

the mass conserved has been studied with simplified advection and shear flow cases and a case capturing the progression of the Rayleigh-Taylor instability. Rudman (1997) reported the superior behavior of the direction split method proposed by Youngs (1982) compared to the Simplified Line Interface Calculation (SLIC) method [Noh and Woodward (1976)], the original VOF method [Hirt and Nichols (1981)] and the flux-corrected transport (FCT) method proposed by Rudman himself. Gopala and van Wachem (2008) considered the Lagrangian Piecewise Linear Interface Construction (PLIC) introduced in Van Wachem and Schouten (2002), the CICSAM [Ubbink (1997)] and the inter-gamma differencing scheme [Jasak and Weller (1995)] to be preferable over the above mentioned FCT method. Xiao et al. (2005) have presented a novel multi-dimensional algebraic VOF method where they used the hyperbolic tangent function to compute the numerical flux for the fluid fraction function. Based on the numerical approach, this version of VOF is named as WLIC (Weighted Linear Interface Calculation). Yokoi (2007) has presented a simplified version of THINC vased WLIC-VOF. The WLIC-VOF has been shown to have same order of accuracy as PLIC-VOF Xiao et al. (2011) although being relatively simpler to implement. Recently Aniszewski et al. (2014) has presented a comprehensive discussion between PLIC and WLIC methods.

Another major direction in recent research on VOF methods has been focused on the interface reconstruction methods. Recently Dyadechko and Shashkov (2005) has presented a higher order formulation of volume tracking approach

similar to VOF. This method, named as MOF (Moment Of Fluid) is further analyzed by Ahn and Shashkov (2009) and others to be applied for general multiphase flow. Some other notable works in reconstruction methods are Aulisa et al. (2007), Diot and François (2016) and Kawano (2016).

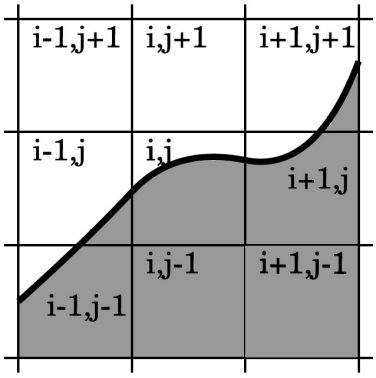

(a) Characteristic function

i-1,j+1	i,j+1	i+1,j+1
0.0	0.0	0.1
i-1,j	i,j	i+1,j
0.1	0.7	0.9
i-1,j-1	i,j-1	i+1,j-1
0.8	1.0	1.0

(b) Volume fraction / Color function

Figure 2: Characteristic Function and Volume Fraction

A brief introduction is given here regarding the numerical formulations used in VOF. Let's consider two phase flow in two-dimensions with fluid A and fluid B. We introduce a characteristic function $\chi(x,y)$ and a volume fraction or color function C_{ij}, defined as

$$\chi(x,y) = \begin{cases} 1, & \text{for the fluid A at the point } (x,y) \\ 0, & \text{for the fluid B at the point } (x,y) \end{cases} \tag{1}$$

$$C_{ij} = \frac{1}{\Delta x \Delta y} \int_0^{\Delta x} \int_0^{\Delta y} \chi(x,y)\, dx dy \tag{2}$$

Note that $\chi(x,y)$ is the value defined at a point (x,y) and is not a value on the

computational grid. On the contrary the color function C_{ij} is defined for each grid cell. Being a continuous function, the value of χ is value 0 or 1, however, the value of C_{ij} is defined as $0 \leq C_{ij} \leq 1$. As we can see, the interface is defined at $\Gamma(x,y)$ where $\chi(x,y)$ changes it's value from 0 to 1 or vice-versa. Also, this $\chi(x,y)$ will be advected as a passive scalar in the flow field i.e.

$$\left.\begin{aligned} \frac{D\chi}{Dt} &= 0 \\ \frac{\partial \chi}{\partial t} + \frac{\partial \chi u}{\partial x} + \frac{\partial \chi v}{\partial y} &= 0 \end{aligned}\right\} \tag{3}$$

χu and χv represents fluxes of χ through the boundaries of control volume. Scardovelli and Zaleski (2000) applied a split approach towards VOF advection. Their formulation calculates fluxes separately along axes and thus, is ideal for parallel implementation. Combining equations from (1), (2) and (3) the split approach gives us:

$$\frac{C_{ij}^{n+1} - C_{ij}^{n}}{\Delta t} = \frac{1}{\Delta x}\left[(F_x)^{n}_{i-\frac{1}{2},j} - (F_x)^{n}_{i+\frac{1}{2},j}\right] + \frac{1}{\Delta y}\left[(F_y)^{n}_{i,j-\frac{1}{2}} - (F_y)^{n}_{i,j+\frac{1}{2}}\right] \tag{4}$$

The terms F_x and F_y represents the flux of χ in x-direction and y-direction along the control volume boundaries. Equation (4) essentially represents the discretized coupling between $\chi(x,y)$ and C_{ij} in a 2D computational framework.

If values of χ_{ij} is known, one can easily use equation (2) to calculate C_{ij} . However, we also need to estimate $\chi(x,y)$ to compute the curvature of the interface which is used to compute the surface tension terms. The problem in

the VOF method is attributed to reconstruction of $\chi(x,y)$ from the volume fraction C_{ij} . As described before, two typical methods to reconstruct $\chi(x,y)$ are the SLIC (simple line interface calculation)[Noh and Woodward (1976)] and the PLIC (piecewise linear interface calculation) method based on works of Youngs (1982). In the SLIC method $\chi(x,y)$ is reconstructed by a line along x or y coordinate as shown in Fig. 3a. An advantage of the SLIC method is the easement of implement. In the PLIC method, χ_i, j is calculated based on an diagonal line/plane as shown in Fig. 3b. The WLIC method as presented in Xiao et al. (2005) and Yokoi (2007) is shown in Fig. 4.

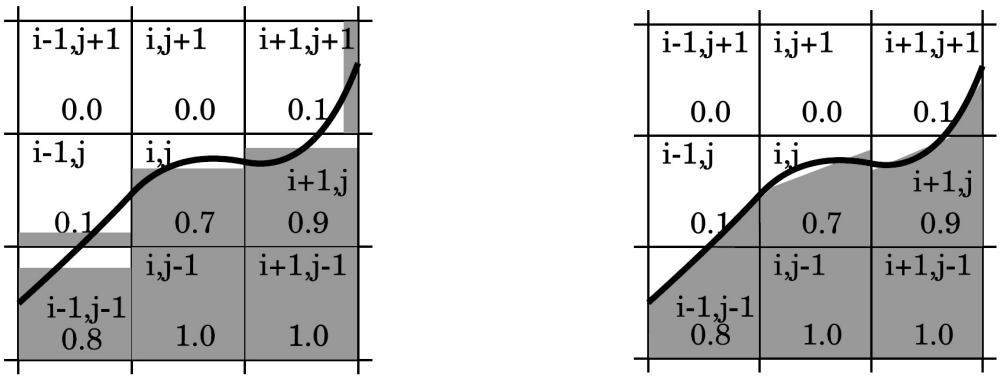

(a) SLIC Reconstruction

(b) PLIC Reconstruction

Figure 3: SLIC and PLIC

In all versions of VOF methods, a modified form of the Navier-Stokes equation is used for the entire domain:

$$\frac{\partial \rho \vec{u}}{\partial t} + \nabla \cdot (\rho \vec{u} \vec{u}) = -\nabla \cdot p + \nabla \cdot (2\mu \vec{E}) + \vec{f}_b + \vec{f}_s \tag{5}$$

where the density and viscosity fields are defined in discrete form as :

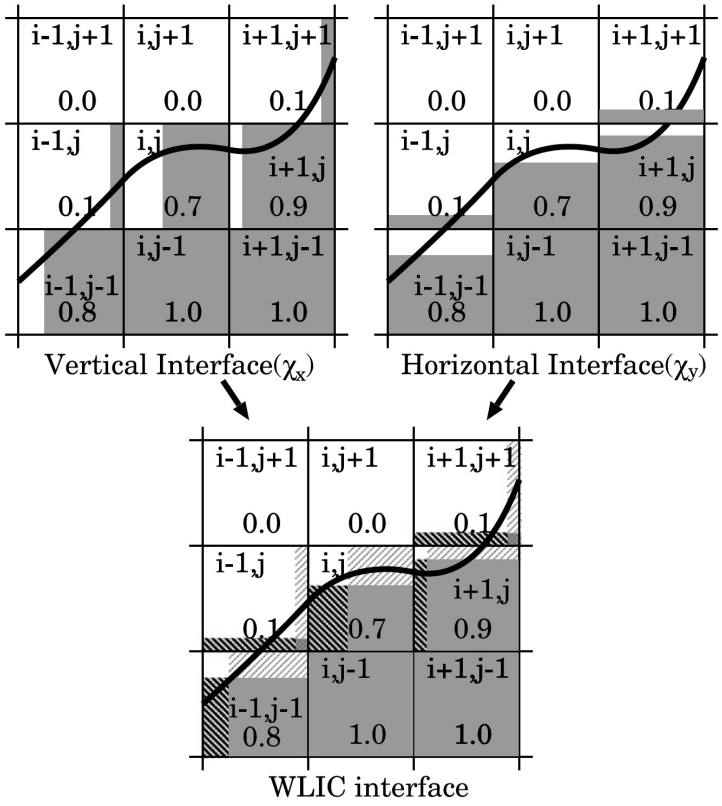

Figure 4: WLIC Reconstruction

$$\left.\begin{aligned} \rho_{ij} &= \rho_A C_{ij} + \rho_B (1 - C_{ij}) \\ \mu_{ij} &= \mu_A C_{ij} + \mu_B (1 - C_{ij}) \end{aligned}\right\} \tag{6}$$

$\vec{u}$, $\vec{f}_b$ and $\vec{E}$ represent the velocity field, body force and the stress tensor respectively. The term $\vec{f}_s$ describes the Laplace pressure acting at the surface of discontinuity and is given by:

$$\vec{f}_s = \sigma \kappa \vec{n} \delta_\Gamma \tag{7}$$

where the interface is indicated by the Dirac delta function δ_Γ. For numerical

implementation, the term $\vec{f}_s$ is replaced by a continuum surface force (CSF):

$$\vec{f}_v = \sigma\kappa\nabla\chi \tag{8}$$

$\vec{f}_v$ tends to $\vec{f}_s$ as the thickness of the interface region tends to zero. The curvature κ is calculated from the approximated characteristic function. This can't be done directly as it leads to large spatial oscillations. Recursive smoothing is employed to get a sufficiently smooth characteristic function, $\hat{\chi}$. The curvature can then be calculated from the smoothed function using:

$$\kappa = \nabla \cdot \vec{n} = \nabla \cdot \left(\frac{\nabla\hat{\chi}}{|\nabla\hat{\chi}|} \right) \tag{9}$$

At the solid boundaries, velocity component normal to the solid wall is zero. At the triple-contact line, Young's law determines the contact angle:

$$cos\theta = \frac{\sigma_{B,s} - \sigma_{A,s}}{\sigma} \tag{10}$$

where $\sigma_{B,s}$ is the fluid B/solid interfacial tension, $\sigma_{A,s}$ is the fluid A/solid interfacial tension. For imposing the contact angle in the simulation, this is equivalent to imposing the boundary condition:

$$\vec{n}_{\Gamma_s} = \vec{n}_s cos\theta + \vec{t}_s sin\theta \tag{11}$$

$\vec{t}_s$ is the unit tangential vector pointing into the fluid A part of the domain.

3.3 Front Tracking Method

The theoretical essence behind the MAC and the VOF methods directly or indirectly influenced many new approaches in the early nineties. Unverdi and Tryggvason (1992) introduced a Front-Tracking method for multiphase flows where the interface was marked by connected massless marker points. The markers are used to advect the material properties (such as density and viscosity) and to compute surface tension, but the rest of computations is done on a fixed grid as in the VOF method. In front tracking methods the interface is defined explicitly, usually by marker particles distributed on interface. The interface is then evolved by solving the ordinary differential equation for each particle:

$$\frac{\partial X}{\partial t} = \vec{u}(X) \qquad \text{for } X \in \Gamma \tag{12}$$

In order to calculate normals and curvatures one needs to keep track of which particle is neighbor to which particle. Particles might move too close together or too far apart, resulting in numerical difficulties. To avoid this, the particles might have to be redistributed along the interface. Since the particles move independently of each other, oscillations in the interface might occur. Some regularizing technique has to be applied to suppress such oscillations. Interpolations also have to be done to interpolate the interface to the fixed grid used for the velocity and pressure. Special care also has to be taken when merging or breakup of interfaces occur. Other examples for the use of marker

points include the Immersed-Boundary Method of Peskin (1977) for one-dimensional elastic fibers in homogeneous viscous fluids and the Vortex-in-Cell method of Tryggvason and Aref (1983) for two-fluid interfaces in a Hele-Shaw cell. Tryggvason and collaborators have used the front tracking scheme to explore a large number of problems.

3.4 Level Set Method

Other numerical methods for multiphase flow includes Level-Set, CIP, and the Phase-Field methods to track fluid interfaces on fixed grids. The Level-Set method was pioneered by Osher and Sethian (1988), but its first use to track fluid interfaces was performed in the the work of Sussman (1994) and Chang et al. (1996) who used level set to simulate the rise of bubbles and the fall of droplets in two-dimensions. An axisymmetric version was applied by Sussman and Smereka (1997) to examine the behavior of bubbles and droplets. Unlike the VOF method, where a discontinuous marker function is advected with the flow, in the Level-Set method a continuous level-set function is used. The interface is then identified with the zero contour of the level-set function. To reconstruct the material properties of the flow a marker/color function is constructed from the level-set function. The marker function is given a smooth transition zone from one fluid to the next, thus increasing the regularity of the interface over the VOF method where the interface is confined to only one grid space. However, this mapping from the level-set function to the marker function requires the level-set function

to maintain the same shape near the interface.To deal with this problem, Sussman (1994) introduced a reinitialization procedure where the level-set function is adjusted accordingly, such that, its value is equal to the shortest distance to the interface at all times. This step was essential to evolve Level-set m/d applicable for fluid-dynamics simulations. Computation of surface tension is performed in the same way as in the continuous surface force technique introduced for VOF methods by Brackbill et al. (1992). The early implementation of the Level-Set method did not conserve mass very well and a number of improvements has been suggested till date. Sussman et al. (1998) and Sussman and Fatemi (1999) modified the level set formulation to improve mass conservation, Sussman et al. (1999) applied level-set with adaptive grid refinement and a hybrid VOF/Level-Set method was developed by Sussman and Puckett (2000).

As described above, in level set method the interface is implicitly defined by a marker function ϕ. The choice of ϕ is made such that, it changes sign at the interface. Thus, it has the following properties:

$$\phi(x,y) = \begin{cases} > 0, & \text{when point } (x,y) \text{ filled with fluid A} \\ = 0, & \text{when point (x,y) is at the interface} \\ < 0, & \text{when point } (x,y) \text{ filled with fluid B} \end{cases} \tag{13}$$

Since the tracked interface is the zero level set of the function ϕ , the interface can

be tracked by solving the following equation:

$$\frac{\partial \phi}{\partial t} + \vec{u} \cdot \nabla \phi = 0 \tag{14}$$

Actually only the normal component of $\vec{u}$ defined by $u_N = \vec{u} \cdot \frac{\nabla \phi}{|\nabla \phi|}$ will affect the movement of the interface Γ. Thus a modified form of equation (14) can be derived for this purpose:

$$\frac{\partial \phi}{\partial t} + u_N \cdot \nabla \phi = 0 \tag{15}$$

ϕ will , as mentioned before, not remain a signed distance function as time evolves. A reinitialization is therefore needed to make sure that ϕ remains a distance function. This reinitialization can also be formulated as a PDE. Given an initial ϕ_0 with the correct position of the zero contour

$$\frac{\partial \phi}{\partial t} + \left[sgn(\phi_0) \right] (|\nabla \phi| - 1) = 0 \tag{16}$$

can be solved to steady state. This was used by Sussman (1994) where the level set method was first used for incompressible two phase flow calculations. In contrast to the characteristic function used in the volume of fluid method, ϕ is smooth across the interface Γ and because of this, standard higher order techniques (e.g ENO, WENO) can be used to solve equation (14).

Similar to VOF methods, a regularization of fluid properties can be done. We now define a Heaviside function $H()$, given by:

$$H(\phi) = \begin{cases} 0, & \phi < 0 \\ \frac{1}{2} + \frac{\phi}{2\epsilon} + \frac{1}{2\pi} sin\left(\frac{\pi\phi}{\epsilon}\right), & -\epsilon \leq \phi \leq \epsilon \\ 1, & \phi > \epsilon \end{cases} \tag{17}$$

The value of ϵ indicates a finite thickness for the interface. Similar to equation (6) we can get

$$\left.\begin{aligned} \rho &= \rho_A H(\phi) + \rho_B (1 - H(\phi)) \\ \mu &= \mu_A H(\phi) + \mu_B (1 - H(\phi)) \end{aligned}\right\} \tag{18}$$

and apply it to the modified navier stokes equation.

The curvature calculation of the interface can be performed based on ϕ similar to the previous calculations in VOF. κ=κ_ϕ is given by:

$$\kappa_\phi = \nabla \cdot \frac{\nabla\phi}{|\nabla\phi|} \tag{19}$$

For 3D, this becomes:

$$\begin{aligned} \kappa_\phi = \left[\frac{1}{|\nabla\phi|^3}\right] (\phi_x^2\phi_{yy} - 2\phi_x\phi_y\phi_{xy} + \phi_y^2\phi_{xx} + \phi_x^2\phi_{zz} - \\ 2\phi_x\phi_z\phi_{xz} + \phi_z^2\phi_{xx} + \phi_y^2\phi_{zz} - 2\phi_x\phi_y\phi_{xy}) \end{aligned} \tag{20}$$

Recently, Enright et al. (2002) presented a modified version of level set method, where markers were used to correct the directed level set function. In

this approach, named as MLS (Marker Level Set) or Particle Level Set (PLS), massless marker particles are utilized to correct the level set function in the under-resolved areas of the interface in order to preserve mass. Two sets (positive and negative) of particles are randomly placed within a band across the interface. Fig. 5 gives a presentation of the approach. It is like a rope-pulley system where the radius of pulley (particles) is defined by :

$$r_p = \begin{cases} r_{max}, & \text{if } S_p\phi(x_p) > r_{max} \\ S_p\phi(x_p), & \text{if } r_{min} \leq S_p(x_p) \leq r_{max} \\ r_{min}, & \text{if } S_p(x_p) < r_{min} \end{cases} \tag{21}$$

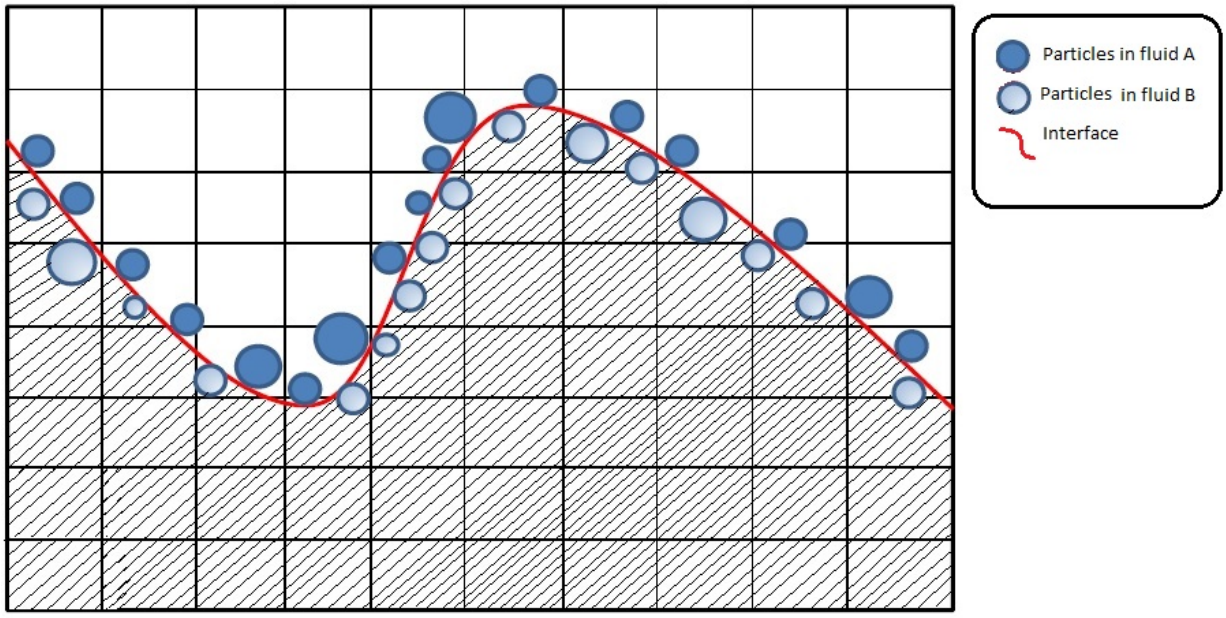

Figure 5: Marker Level Set/ Particle Level set

Here, value of the signed function S_p is +1 or -1 depending of which side of interface the particle is located. After temporal evolution, a check is performed

to identify whether any particle has switch side with respect to interface. for each escaped particle, a new level set function is computed as $\phi_p = S_p(r_p - |x - x_p|)$. Afterwards, ϕ^+ and $\phi^-$are calculated as:

$$\left.\begin{aligned} \phi^+ &= \max(\phi_p, \phi_A) \qquad \text{for fluid A side} \\ \phi^+ &= \max(\phi_p, \phi_B) \qquad \text{for fluid B side} \end{aligned}\right\} \tag{22}$$

Finally the final correction is performed as:

$$\phi = \begin{cases} \phi^+, & \text{if } |\phi^+| \leq |\phi^-| \\ r_{min}, & \text{if } |\phi^+| > |\phi^-| \end{cases} \tag{23}$$

The correction step in MLS is further discussed and improved by Gaudlitz and Adams (2008), Wang et al. (2009) and others.

3.5 CIP and Phase Field Method

The Constrained Interpolated Propagation (CIP) method was introduced by Takewaki et al. (1985). In the CIP method the transition from one fluid to another is formulated by a cubic polynomial. Both the marker function and its derivative are then updated to advect the interface. In addition to the simulation of two-fluid problems, this method has been used for a number of more complex applications, such as those involving floating solids by Yabe et al. (2001).

The Phase-Field approach was introduced by [Kobayashi (1992, 1993)] to model solidification. In the Phase-Field method the governing equations are

modified to describe the dynamics of the smoothed region between the different fluids in a thermodynamically consistent way. Computationally, the overall effect of the modification is to provide an "anti-diffusive" term that keeps the interface reasonably sharp. Although there are considerable similarities between Phase-Field and Level-Set methods, the fundamental ideas behind these two methods are very different. In the Level Set method the smoothness of the phase boundary is artificial and introduced for numerical reasons only. On the contrary, in Phase-Field methods the transition zone is real, although it is made much thicker than it should be for numerical reasons. So in phase field model, we apply proper thermodynamic conditions in an artificially thick interface. For the motion of two immiscible fluids with a sharp interface, this condition leads to additional resolution requirement that is more stringent than for other "one-fluid" methods. The Phase-Field methods are advantageous for problems where small-scale physics are of high importance, since it is difficult to do so in the sharp interface limit. Compared to VOF, Front-Tracking m/d or Level Set method, use of Phase-Field approach for fluid dynamic simulations is relatively limited [Jacqmin (1999); Jamet et al. (2001)].

3.6 Sharp-Interface Methods

In all the "one-fluid" methods described above, the accuracy is generally compromised due to the numerical thickness of the interface. Therefore several attempts has been made to treat the interface as "fully sharp". Glimm and his

1. Interface Capturing Methods [Quirk (1994)]
2. Interface Tracking Methods
   A. Front Tracking Methods [Unverdi and Tryggvason (1992)]
   B. Volume Tracking Methods
      I. Marker and Cell (MAC) [Hirt and Nichols (1981)]
      II. Volume Of Fluid (VOF)
         a) Simple Line Interface Calculation (SLIC) [Noh and Woodward (1976)]
         b) Piecewise Linear Interface Calculation (PLIC) [Youngs (1982)]
         c) Weighted Line Interface Calculation (WLIC) [Xiao et al. (2005)]
         d) Flux Corrected Transport (FCT) [Rudman (1997)]
         e) Constrained Interpolation Profile (CIP) [Takewaki et al. (1985)]
      III. Moment Of Fluid (MOF) [Dyadechko and Shashkov (2005)]
      IV. Level Set (LS) [Osher and Sethian (1988)]
      V. Hybrid Methods
         a) Coupled Level-Set Volume-Of-Fluid (CLSVOF) [Sussman and Puckett (2000)]
         b) Marker Level-Set (MLS) [Enright et al. (2002)]
   C. Phase-Field Methods [Kobayashi (1992)]

Figure 6: Classification of numerical methods for multiphase flow

collaborators [Glimm et al. (2001)] applied local modification to the grids near the interface in such a way that the interface coincided with a cell boundary. Another example is the "cut-cell" methods which is used to include complex bodies in simulations of inviscid flows by Quirk (1994) and Powell (1998).

In the "ghost fluid" method introduced by Fedkiw et al. (1999) the interface is marked by advecting a level-set function. Fictitious values are assigned to grid points near the interface for the numerical approximations of derivatives (i.e where the finite difference stencil involves values from both sides of the interface). These fictitious values are obtained by extrapolation and a there exists different approaches to do so.

Udaykumar et al. (2001) represented complex solid boundaries on a regular grid by merging cells near the interface and using polynomial fitting to find field values at the interface. This method has been extended and well documented in Marella et al. (2005), Liu et al. (2005) and Yang and Udaykumar (2005).

The "Immersed Interface" method of Lee and Leveque (2003) modifies the numerical approximations near the interface by explicitly incorporating jump condition across the interface into finite difference equations. While this is easily done for relatively simple jump conditions, the simplicity is compromised for complex situations. As a result Lee and Leveque (2003) limited their implementation for fluids with the same viscosity.

A classification of the reviewed methods in tabulated form is presented in Fig (6).

3.7 Adaptive Mesh

One of the major developments in the field of numerical multiphase flow is the application of adaptive mesh refinement (AMR). As noted previously the all conventional numerical approaches suffer from accuracy issues due to the numerical thickness of interface. AMR method counters these inaccuracies by dynamically refining the mesh near the interface. There exists a large variety of approaches to introduce mesh adaptivity which differ in many aspects such as mesh topology, refinement criteria and data structure management. A complete review is beyond the scope of this proposal. Popinet (2003) and Fuster et al. (2009) applied the octree type adaptive mesh framework for VOF method. Recently Tan (2016) used a modified version of the same numerical framework to analyze free-surfaces flow problems related to thermal inkjet technology. Laurmaa et al. (2016) has developed a semi-Lagrangian VOF approach in the adaptive mesh framework and used it to study free surface flow. As mentioned previously Sussman et al. (1999) applied AMR for level-set method. Recent works in this context include Losasso et al. (2006) and Kolomenskiy et al. (2016). Application of adaptive mesh for front tracking method and phase field method can be found in Pivello et al. (2014) and Ceniceros et al. (2010) respectively.

4 Research Plan

The proposed research can be divided into three major parts:

1. Development of a numerical solver capable to effectively capture the interfacial dynamics in two-phase flow.

2. Investigation of different drop-impact problems and analysis of the corresponding interfacial dynamics.

3. Preparation of regime maps for different cases and to provide a conclusive explanation for the transition mechanism from coalescence to splashing.

The selection of interface capturing/tracking method must be done first. Afterwards attention will be given for the preparation and validation of a numerical solver with desired efficiency. For validation of the solver, we intend to use some classical problems (e.g Rayleigh Taylor Instability, Rising Bubble, Kelvin Helmholtz Instability) It is expected that one and half year will be needed to complete this task properly.

Afterwards the solver will be used to perform direct numerical simulation for drop impact problem. as noted earlier, we intend to consider the effect of different physical parameters including the shape of drop, the temperature difference between drop and fluid surface. Considering the access to a good computational platform this part can be completed within one year.

The final part (regime mapping) of this suggested research is expected to take atleast two years. However, it is highly recommended that we start with available

numerical facilities for this part (e.g Gerris or OpenFOAM). By doing so, results for some cases (e.g for cases without heat transfer) can be computed before completion of stage one. These results can be used alongwith the expected results from the developed solver with more complex physical conditions to provide a consistent regime map for the transition. Thus this part of the research can be started alongwith part one of this proposed work.

5 Expected Results

The expected results of this work can be summerized as follows:-

1. A three dimentional multiphase solver
2. Detailed numerical investigation of Rayleigh jet formation
3. A well resolved regime map to represent the transition from drop coalescence to splashing

References

Agbaglah, G., Josserand, C., and Zaleski, S. (2013). Longitudinal instability of a liquid rim. *Physics of Fluids*, 25(2).

Agbaglah, G., Thoraval, M.-J., Thoroddsen, S. T., Zhang, L. V., Fezzaa, K., and Deegan, R. D. (2015). Drop impact into a deep pool: vortex shedding and jet formation. *Journal of Fluid Mechanics*, 764:R1.

Ahn, H. and Shashkov, M. (2009). Adaptive moment-of-fluid method. *Journal of Computational Physics*, 228(8):2792–2821.

Aniszewski, W., MÃl'nard, T., and Marek, M. (2014). Volume of fluid (vof) type advection methods in two-phase flow: A comparative study. *Computers and Fluids*, 97:52–73.

Ashgriz, N. and Poo, J. Y. (1991). FLAIR: Flux line-segment model for advection and interface reconstruction. *Journal of Computational Physics*, 93(2):449–468.

Aulisa, E., Manservisi, S., Scardovelli, R., and Zaleski, S. (2007). Interface reconstruction with least-squares fit and split advection in three-dimensional Cartesian geometry. *Journal of Computational Physics*, 225(2):2301–2319.

Bolleddula, D. A., Berchielli, A., and Aliseda, A. (2010). Impact of a heterogeneous liquid droplet on a dry surface: Application to the pharmaceutical industry. *Advances in Colloid and Interface Science*, 159(2):144–159.

Brackbill, J. U., Kothe, D. B., and Zemach, C. (1992). A continuum method for modeling surface tension. *Journal of Computational Physics*, 100(2):335–354.

Castillo-Orozco, E., Davanlou, A., Choudhury, P. K., and Kumar, R. (2015). Droplet impact on deep liquid pools: Rayleigh jet to formation of secondary droplets. *Physical Review E - Statistical, Nonlinear, and Soft Matter Physics*, 92(5).

Ceniceros, H. D., Nós, R. L., and Roma, A. M. (2010). Three-dimensional, fully adaptive simulations of phase-field fluid models. *Journal of Computational Physics*, 229(17):6135–6155.

Chan, R. K. and Street, R. L. (1970). A computer study of finite-amplitude water waves. *Journal of Computational Physics*, 6(1):68–94. Cited By :183.

Chang, Y. C., Hou, T. Y., Merriman, B., and Osher, S. (1996). A level set formulation of Eulerian interface capturing methods for incompressible fluid flows. *Journal of Computational Physics*, 124(2):449–464.

Chapman, R. and Plesset, M. (1972). Nonlinear effects in the collapse of a nearly spherical cavity in a liquid. *J Basic Eng Trans ASME*, 94 Ser D(1):142–146. Cited By :28.

Chen, S., Johnson, D. B., Raad, P. E., and Fadda, D. (1997). The surface marker and micro cell method. *International Journal for Numerical Methods in Fluids*, 25(7):749–778.

Cole, D. (2007). *The splashing morphology of liquid-liquid impacts*. PhD thesis, James Cook University.

Cossali, G. E., Coghe, a., and Marengo, M. (1997). The impact of a single drop on a wetted solid surface. *Experiments in Fluids*, 22(6):463–472.

Daly, B. J. (1969a). Numerical study of the effect of surface tension on interface instability. *Physics of Fluids*, 12(7):1340–1354. Cited By :65.

Daly, B. J. (1969b). A technique for including surface tension effects in hydrodynamic calculations. *Journal of Computational Physics*, 4(1):97–117. Cited By :61.

De Bar, R. (1974). Fundamentals of the KRAKEN code. *Technical Report*.

Deegan, R. D., Brunet, P., and Eggers, J. (2007). Complexities of splashing. *Nonlinearity*, 21(1):C1–C11.

Diot, S. and François, M. M. (2016). An interface reconstruction method based on an analytical formula for 3D arbitrary convex cells. *Journal of Computational Physics*, 305:63–74.

Driscoll, M. M. and Nagel, S. R. (2011). Ultrafast interference imaging of air in splashing dynamics. *Physical Review Letters*, 107(15).

Duchemin, L. and Josserand, C. (2011). Curvature singularity and film-skating during drop impact. *Physics of Fluids*, 23(9).

Dyadechko, V. and Shashkov, M. (2005). Interface tracking capabilities of the inter-gamma differencing scheme. Technical report, Los Alamos National Laboratory.

Edgerton, H. and Killian, J. (1939). *Flash!: Seeing the unseen by ultra high-speed photography*. Boston Hale Cushman and Flint.

Enright, D., Fedkiw, R., Ferziger, J., and Mitchell, I. (2002). A hybrid particle level set method for improved interface capturing. *Journal of Computational Physics*, 183(1):83–116.

Esmailizadeh, L. and Mesler, R. (1986). Bubble entrainment with drops. *Journal of Colloid And Interface Science*, 110(2):561–574.

Fedkiw, R. P., Aslam, T., Merriman, B., and Osher, S. (1999). A Non-oscillatory Eulerian Approach to Interfaces in Multimaterial Flows (the Ghost Fluid Method). *Journal of Computational Physics*, 152(2):457–492.

Foote, G. (1973). A numerical method for studying liquid drop behavior: Simple oscillation. *Journal of Computational Physics*, 11(4):507–530. Cited By :50.

Foote, G. B. (1975). Water drop rebound problem: Dynamics of collision. Cited By :46.

Franz, G. J. (1959). Splashes as sources of sound in liquids. *The Journal of the Acoustical Society of America*, 31(8):1080–1096.

Fuster, D., Bagué, A., Boeck, T., Le Moyne, L., Leboissetier, A., Popinet, S., Ray, P., Scardovelli, R., and Zaleski, S. (2009). Simulation of primary atomization with an octree adaptive mesh refinement and VOF method. *International Journal of Multiphase Flow*, 35(6):550–565.

Gaudlitz, D. and Adams, N. (2008). On improving mass-conservation properties of the hybrid particle-level-set method. *Computers and Fluids*, 37(10):1320–1331.

Glimm, J., Grove, J. W., Li, X. L., Oh, W., and Sharp, D. H. (2001). A Critical Analysis of Rayleigh-Taylor Growth Rates. *Journal of Computational Physics*, 169(2):652–677.

Gopala, V. R. and van Wachem, B. G. M. (2008). Volume of fluid methods for immiscible-fluid and free-surface flows. *Chemical Engineering Journal*, 141(1-3):204–221.

Gueyffier, D. and Zaleski, S. (1998). Formation de digitations lors de l'impact d'une goutte sur un film liquide. *Comptes Rendus de l'Academie de Sciences - Serie IIb: Mecanique, Physique, Chimie, Astronomie*, 326(12):839–844.

Harlow, F. H. and Shannon, J. P. (1967). The splash of a liquid drop. *Journal of Applied Physics*, 38(10):3855–3866. Cited By :219.

Harlow, F. H. and Welch, J. E. (1965). Numerical calculation of time-dependent viscous incompressible flow of fluid with free surface. *Physics of Fluids*, 8(12):2182–2189. Cited By :3037.

Harlow, F. H. and Welch, J. E. (1966). Numerical study of large-amplitude free-surface motions. *Physics of Fluids*, 9(5):842–851. Cited By :113.

Hicks, P. D. and Purvis, R. (2011). Air cushioning in droplet impacts with liquid layers and other droplets. *Physics of Fluids*, 23(6).

Hirt, C. W. and Nichols, B. D. (1981). Volume of fluid (VOF) method for the dynamics of free boundaries. *Journal of Computational Physics*, 39(1):201–225.

Hulse-Smith, L., Mehdizadeh, N. Z., and Chandra, S. (2005). Deducing drop size and impact velocity from circular bloodstains. *Journal of Forensic Sciences*, 50(1):54–63.

Jacqmin, D. (1999). Calculation of Two-Phase Navier-Stokes Flows Using Phase-Field Modeling. *Journal of Computational Physics*, 155(1):96–127.

Jamet, D., Lebaigue, O., Coutris, N., and Delhaye, J. M. (2001). The Second Gradient Method for the Direct Numerical Simulation of Liquid-Vapor Flows with Phase Change. *Journal of Computational Physics*, 169(2):624–651.

Jasak, H. and Weller, H. (1995). Interface tracking capabilities of the inter-gamma differencing scheme. Technical report, Imperial College of Science, Technology and Medicine.

Josserand, C. and Zaleski, S. (2003). Droplet splashing on a thin liquid film. *Physics of Fluids*, 15(6):1650–1657.

Kawano, A. (2016). A simple volume-of-fluid reconstruction method for three-dimensional two-phase flows. *Computers and Fluids*, 134-135:130–145.

Kim, J. (2007). Spray cooling heat transfer: The state of the art. *International Journal of Heat and Fluid Flow*, 28(4):753–767.

Knock, C. and Davison, M. (2007). Predicting the position of the source of blood stains for angled impacts. *Journal of Forensic Sciences*, 52(5):1044–1049.

Kobayashi, R. (1992). Simulations of three dimensional dendrites. *Pattern Formation in Complex Dissipative Systems*, pages 121–128.

Kobayashi, R. (1993). Modeling and numerical simulations of dendritic crystal growth. *Physica D: Nonlinear Phenomena*, 63(3-4):410–423.

Kolinski, J. M., Rubinstein, S. M., Mandre, S., Brenner, M. P., Weitz, D. A., and Mahadevan, L. (2012). Skating on a film of air: Drops impacting on a surface. *Physical Review Letters*, 108(7).

Kolomenskiy, D., Nave, J.-C., and Schneider, K. (2016). Adaptive Gradient-Augmented Level Set Method with Multiresolution Error Estimation. *Journal of Scientific Computing*, 66(1):116–140.

Krechetnikov, R. (2010). Stability of liquid sheet edges. *Physics of Fluids*, 22(9).

Krechetnikov, R. and Homsy, G. M. (2009). Crown-forming instability phenomena in the drop splash problem. *Journal of Colloid and Interface Science*, 331(2):555–559.

Lafaurie, B., Nardone, C., Scardovelli, R., Zaleski, S., and Zanetti, G. (1994). Modelling Merging and Fragmentation in Multiphase Flows with SURFER. *Journal of Computational Physics*, 113(1):134–147.

Laurmaa, V., Picasso, M., and Steiner, G. (2016). An octree-based adaptive semi-Lagrangian VOF approach for simulating the displacement of free surfaces. *Computers and Fluids*, 131:190–204.

Lee, L. and Leveque, R. J. (2003). An immersed interface method for incompressible Navier-Stokes equations. *SIAM Journal on Scientific Computing*, 25(3):832–856.

Liow, J.-L. and Cole, D. E. (2007). Bubble entrapment mechanisms during the impact of a water drop. *16th Australasian Fluid Mechanics Conference (AFMC)*, pages 866–869.

Liu, H., Krishnan, S., Marella, S., and Udaykumar, H. S. (2005). Sharp interface Cartesian grid method II: A technique for simulating droplet interactions with surfaces of arbitrary shape. *Journal of Computational Physics*, 210(1):32–54.

Liu, Y., Tan, P., and Xu, L. (2013). Compressible air entrapment in high-speed drop impacts on solid surfaces. *Journal of Fluid Mechanics*, 716(November 2012):R9.

Losasso, F., Fedkiw, R., and Osher, S. (2006). Spatially adaptive techniques for level set methods and incompressible flow. *Computers and Fluids*, 35(10):995–1010.

Marella, S., Krishnan, S., Liu, H., and Udaykumar, H. S. (2005). Sharp interface Cartesian grid method I: An easily implemented technique for 3D moving boundary computations. *Journal of Computational Physics*, 210(1):1–31.

Marston, J., Thoroddsen, S., Ng, W., and Tan, R. (2010). Experimental study of liquid drop impact onto a powder surface. *Powder Technology*, 203(2):223–236.

Mehdi-Nejad, V., Mostaghimi, J., and Chandra, S. (2003). Air bubble entrapment under an impacting droplet. *Physics of Fluids*, 15(1):173–183.

Mitchell, T. M. and Hammitt, F. G. (1973). Asymmetric cavitation bubble collapse. *Journal of Fluids Engineering, Transactions of the ASME*, 95 Ser I(1):29–37. Cited By :29.

Moreira, A. L. N., Moita, A. S., and Panão, M. R. (2010). Advances and challenges in explaining fuel spray impingement: How much of single droplet impact research is useful? *Progress in Energy and Combustion Science*, 36(5):554–580.

Morton, D., Rudman, M., and Liow, J.-L. (2000). An investigation of the flow regimes resulting from splashing drops. *Physics of Fluids*, 12(4):747.

Mundo, C., Sommerfeld, M., and Tropea, C. (1995). Droplet-wall collisions: Experimental studies of the deformation and breakup process. *International Journal of Multiphase Flow*, 21(2):151–173.

Noh, W. F. and Woodward, P. (1976). SLIC (simple line interface calculation). *Lecture Notes in Physics*, 59:330–340.

Osher, S. and Sethian, J. A. (1988). Fronts propagating with curvature-dependent speed: Algorithms based on Hamilton-Jacobi formulations. *Journal of Computational Physics*, 79(1):12–49.

Palacios, J., Hernández, J., Gómez, P., Zanzi, C., and López, J. (2012). On the impact of viscous drops onto dry smooth surfaces. *Experiments in Fluids*, 52(6):1449–1463.

Peck, B. and Sigurdson, L. (1994). The three-dimensional vortex structure of an impacting water drop. *Physics of Fluids*, 6(2):564–576.

Peskin, C. S. (1977). Numerical analysis of blood flow in the heart. *Journal of Computational Physics*, 25(3):220–252.

Pivello, M. R., Villar, M. M., Serfaty, R., Roma, A. M., and Silveira-Neto, A. (2014). A fully adaptive front tracking method for the simulation of two phase flows. *International Journal of Multiphase Flow*, 58:72–82.

Popinet, S. (2003). Gerris: A tree-based adaptive solver for the incompressible Euler equations in complex geometries. *Journal of Computational Physics*, 190(2):572–600.

Popinet, S. (2009). An accurate adaptive solver for surface-tension-driven interfacial flows. *Journal of Computational Physics*, 228(16):5838–5866.

Powell, K. (1998). Solution of the Euler equations on solution-adaptive Cartesian grids. *In Computational Fluid Dynamics Reviews 1998*, 1:65–92.

Prosperetti, A. and Oguz, H. N. (1993). The impact of drops on liquid surfaces and the underwater noise of rain. *Annual Review of Fluid Mechanics*, 25(1):577–602.

Pumphrey, H. C., Crum, L. A., and Bjørnø, L. (1989). Underwater sound produced by individual drop impacts and rainfall. *The Journal of the Acoustical Society of America*, 85(4):1518–1526.

Pumphrey, H. C. and Elmore, P. A. (1990). The entrainment of bubbles by drop impacts. *Journal of Fluid Mechanics*, 220(-1):539–567.

Quirk, J. J. (1994). An alternative to unstructured grids for computing gas dynamic flows around arbitrarily complex two-dimensional bodies. *Computers and Fluids*, 23(1):125–142.

R. Davidson, M. (2002). Spreading of an inviscid drop impacting on a liquid film. *Chemical Engineering Science*, 57(17):3639–3647.

Ray, B., Biswas, G., and Sharma, A. (2015). Regimes during liquid drop impact on a liquid pool. *Journal Of Fluid Mechanics*, 768:492–523.

Rein, M. (1993). Phenomena of liquid drop impact on solid and liquid surfaces. *Fluid Dynamics Research*, 12(2):61–93.

Rein, M. (1996). The transitional regime between coalescing and splashing drops. *Journal of Fluid Mechanics*, 306(-1):145.

Renardy, Y. and Renardy, M. (2002). PROST: A parabolic reconstruction of surface

tension for the volume-of-fluid method. *Journal of Computational Physics*, 183(2):400–421.

Rider, W. J. and Kothe, D. B. (1998). Reconstructing volume tracking. *Journal of Computational Physics*, 141(2):112–152. Cited By :822.

Rioboo, R., Bauthier, C., Conti, J., Voué, M., and De Coninck, J. (2003). Experimental investigation of splash and crown formation during single drop impact on wetted surfaces. *Experiments in Fluids*, 35(6):648–652.

Rioboo, R., Tropea, C., and Marengo, M. (2001). Outcomes from a drop impact on solid surfaces. *Atomization and Sprays*, 11(2):155–165.

Rossi, V. and Caffi, T. (2012). The role of rain in dispersal of the primary inoculum of Plasmopara viticola. *Phytopathology*, 102(2):158–65.

Rudman, M. (1997). Volume-tracking methods for interfacial flow calculations. *International Journal for Numerical Methods in Fluids*, 24(7):671–691.

Sawan, M. E. and Carbon, M. W. (1975). A review of spray-cooling and bottom-flooding work for lwr cores. *Nuclear Engineering and Design*, 32(2):191–207.

Scardovelli, R. and Zaleski, S. (2000). Analytical Relations Connecting Linear Interfaces and Volume Fractions in Rectangular Grids. *Journal of Computational Physics*, 164(1):228–237.

Sigler, J. and Mesler, R. (1990). The behavior of the gas film formed upon

drop impact with a liquid surface. *Journal of Colloid And Interface Science*, 134(2):459–474.

Smith, F., Li, L., and Wu, G. X. (2003). Air cushioning with a lubrication/inviscid balance. *Journal of Fluid Mechanics*, 482:291–318.

Stow, C. D. and Hadfield, M. G. (1981). An experimental investigation of fluid flow resulting from the impact of a water drop with an unyielding dry surface. *Proceedings of the Royal Society A: Mathematical, Physical and Engineering Sciences*, 373(1755):419–441.

Sussman, M. (1994). A level set approach for computing solutions to incompressible two-phase flow. *Journal of Computational Physics*, 114(1):146–159.

Sussman, M., Almgren, A. S., Bell, J. B., Colella, P., Howell, L. H., and Welcome, M. L. (1999). An Adaptive Level Set Approach for Incompressible Two-Phase Flows. *Journal of Computational Physics*, 148(1):81–124.

Sussman, M. and Fatemi, E. (1999). Efficient, interface-preserving level set redistancing algorithm and its application to interfacial incompressible fluid flow. *SIAM Journal on Scientific Computing*, 20(4):1165–1191.

Sussman, M., Fatemi, E., Smereka, P., and Osher, S. (1998). An improved level set method for incompressible two-phase flows. *Computers and Fluids*, 27(5-6):663–680.

Sussman, M. and Puckett, E. G. (2000). A Coupled Level Set and Volume-of-Fluid Method for Computing 3D and Axisymmetric Incompressible Two-Phase Flows. *Journal of Computational Physics*, 162(2):301–337.

Sussman, M. and Smereka, P. (1997). Axisymmetric free boundary problems. *Journal of Fluid Mechanics*, 341:269–294.

Takewaki, H., Nishiguchi, A., and Yabe, T. (1985). Cubic interpolated pseudo-particle method (CIP) for solving hyperbolic-type equations. *Journal of Computational Physics*, 61(2):261–268.

Tan, H. (2016). An adaptive mesh refinement based flow simulation for free-surfaces in thermal inkjet technology. *International Journal of Multiphase Flow*, 82:1–16.

Thoroddsen, S. and Sakakibara, J. (1998). Evolution of the fingering pattern of an impacting drop. *Physics of Fluids*, 10(6):1359.

Thoroddsen, S., Thoraval, M.-J., Takehara, K., and Etoh, T. G. (2012). The breakup of thin air films caught under impacting drops. In *65th Annual Meeting of the APS Division of Fluid Dynamics*, volume 57.

Thoroddsen, S. T. (2002). The ejecta sheet generated by the impact of a drop. *Journal of Fluid Mechanics*, 451:373–381.

Thoroddsen, S. T., Etoh, T. G., and Takehara, K. (2003). Air entrapment under an impacting drop. *Journal of Fluid Mechanics*, 478:125–134.

Thoroddsen, S. T., Etoh, T. G., and Takehara, K. (2008). High-Speed Imaging of Drops and Bubbles. *Annual Review of Fluid Mechanics*, 40:257–285.

Tryggvason, G. and Aref, H. (1983). Numerical experiments on Hele Shaw flow with a sharp interface. *Journal of Fluid Mechanics*, 136:1–30.

Tryggvason, G., Scardovelli, R., and Zaleski, S. (2011). *Direct Numerical Simulations of Gas-Liquid Multiphase Flows*.

Ubbink, O. (1997). *Numerical prediction of two fluid systems with sharp interfaces*. PhD thesis, Imperial College London.

Udaykumar, H. S., Mittal, R., Rampunggoon, P., and Khanna, A. (2001). A sharp interface Cartesian grid method for simulating flows with complex moving boundaries. *Journal of Computational Physics*, 174(1):345–380.

Unverdi, S. O. and Tryggvason, G. (1992). A front-tracking method for viscous, incompressible, multi-fluid flows. *Journal of Computational Physics*, 100(1):25–37.

Van Wachem, B. G. M. and Schouten, J. C. (2002). Experimental validation of 3-D Lagrangian VOF model: Bubble shape and rise velocity. *AIChE Journal*, 48(12):2744–2753.

Villermaux, E. and Clanet, C. (2002). Life of a flapping liquid sheet. *Journal of Fluid Mechanics*, 462:341–363.

Wang, Z., Yang, J., and Stern, F. (2009). An improved particle correction procedure for the particle level set method. *Journal of Computational Physics*, 228(16):5819–5837.

Wanninkhof, R., Asher, W. E., Ho, D. T., Sweeney, C., and McGillis, W. R. (2009). Advances in quantifying air-sea gas exchange and environmental forcing. *Annual review of marine science*, 1:213–244.

Weiss, D. A. and Yarin, A. L. (1999). Single drop impact onto liquid films: neck distortion, jetting, tiny bubble entrainment, and crown formation. *Journal of Fluid Mechanics*, 385:229–254.

Worthington, a. M. (1876). A Second Paper on the Forms Assumed by Drops of Liquids Falling Vertically on a Horizontal Plate. *Proceedings of the Royal Society of London*, 25(171-178):498–503.

Worthington, A. M. (1877). A second paper on the forms assumed by drops of liquids falling vertically on a horizontal plate. *Proceedings of the Royal Society of London*, 25(171-178):498–503.

Worthington, A. M. (1882). On impact with a liquid surface. *Proceedings of the Royal Society of London*, 34(220-223):217–230.

Worthington, A. M. (1895). *The title of the work*. London.

Worthington, A. M. (1908). *A study of splashes*. Longmans, Green, and co.

Xiao, F., Honma, Y., and Kono, T. (2005). A simple algebraic interface capturing scheme using hyperbolic tangent function. *International Journal for Numerical Methods in Fluids*, 48(9):1023–1040.

Xiao, F., Ii, S., and Chen, C. (2011). Revisit to the {THINC} scheme: A simple algebraic {VOF} algorithm. *Journal of Computational Physics*, 230(19):7086–7092.

Xu, L., Zhang, W. W., and Nagel, S. R. (2005). Drop splashing on a dry smooth surface. *Physical Review Letters*, 94(18).

Yabe, T., Xiao, F., and Utsumi, T. (2001). The Constrained Interpolation Profile Method for Multiphase Analysis. *Journal of Computational Physics*, 169(2):556–593.

Yang, Y. and Udaykumar, H. S. (2005). Sharp interface Cartesian grid method III: Solidification of pure materials and binary solutions. *Journal of Computational Physics*, 210(1):55–74.

Yarin, A. L. (2006). Drop Impact Dynamics: Splashing, Spreading, Receding, Bouncing... *Annual Review of Fluid Mechanics*, 38:159–192.

Yokoi, K. (2007). Efficient implementation of thinc scheme: A simple and practical smoothed vof algorithm. *Journal of Computational Physics*, 226(2):1985–2002.

Youngs, D. L. (1982). Time-dependent multi-material flow with large fluid distortion. *Numerical Methods for Fluid Dynamics*, pages 273–285.

Zhang, L. V., Brunet, P., Eggers, J., and Deegan, R. D. (2010). Wavelength selection in the crown splash. *Physics of Fluids*, 22(12).

Zhang, L. V., Toole, J., Fezzaa, K., and Deegan, R. D. (2012). Evolution of the ejecta sheet from the impact of a drop with a deep pool. *Journal of Fluid Mechanics*, 690:5–15.